Supplement of Atmos. Chem. Phys., 19, 499–521, 2019
https://doi.org/10.5194/acp-19-499-2019-supplement

Atmospheric Chemistry and Physics
Open Access
EGU

Supplement of

Volatile organic compounds and ozone in Rocky Mountain National Park during FRAPPÉ

Katherine B. Benedict et al.

Correspondence to: Katherine B. Benedict (katherine.benedict@colostate.edu)

More detailed methods:

In situ GC

The VOC analytical system was similar to those used in previous studies (Abeleira et al., 2017; Sive et al., 2005) and utilized a Qdrive 2s102K cryocooler (Chart, Inc., Troy, NY) that was capable of cooling a sample enrichment loop from 100 °C to -180 °C in 25 minutes for sample concentration. The loop was made from a 4 inch × 3/16 inch piece of stainless steel tubing and filled with 1 mm diameter deactivated glass beads (Ohio Valley, Marietta, OH) to provide an inert area for sample concentration during the trapping stage. The loop was heated to ~100 °C during the desorption, injection, and bake out stages of the system.

The trapping procedure was initiated when the sample enrichment loop reached its initial set point temperature (-180 °C). A 1000 cm^3 aliquot of ambient air was sampled through a heated stainless steel inlet line (70 °C) to remove O_3 prior to the sample passing through the enrichment loop at a rate of 200 cm^3 min^{-1}. After the ambient air trapping procedure was completed, 100 cm^3 of ultra-high purity (UHP) helium was passed through the loop at a rate of 100 cm^3 min^{-1}. The helium sweep was used to remove any residual O_3, because condensed phase chemistry with O_3 may occur before or during desorption (Koppmann et al., 1995). After the helium sweep was completed, the sample enrichment loop was isolated, and rapidly heated to 100 °C. Once the desorption temperature was reached, the sample was injected, and the GCs were triggered to start the temperature programs. UHP helium carrier gas flushed the contents of the sample enrichment loop through a 0.53 mm i.d. Silonite-coated transfer line to the splitter box. At the splitter box, the sample was quantitatively and reproducibly split into four sample sub-streams. Each of the four sub-streams was transferred to a separate GC separation column/detector pair.

Two Shimadzu GC-17A gas chromatographs (Shimadzu Scientific, Columbia, MD) each housed two different separation columns. One 50 m × 0.53 mm i.d., 10 µm film thickness CP-Al_2O_3/Na_2SO_4 PLOT column, one 60 m × 0.32 mm i.d., 1µm film thickness VF-1ms column, one 60 m × 0.25 mm i.d., 3µm film thickness CP-PoraBond Q column, and one 60 m × 0.25 mm i.d., 1.0 µm film thickness VF-1701 column (Varian Inc.) were used for trace gas separation. The PLOT, VF-1ms, and PoraBond Q columns were each connected to a Flame Ionization Detector (FID) for analysis of C_2-C_7 and C_6-C_{10} non-methane hydrocarbons (NMHC), and selected oxidized VOCs (OVOCs: methanol, ethanol, acetaldehyde, acetone and

MEK) measurements, respectively. The VF-1701 column was plumbed into an Electron Capture Detector (ECD) and used for measuring C_1-C_2 halocarbons and C_1-C_5 alkyl nitrates.

Two different whole air standards were alternately analysed every 10 samples throughout the campaign. The measurement precision, represented by the relative standard deviation (RSD) of the peak areas for each compound in the standards, was 1-8% for the NMHCs, 3-11% for halocarbons, and 3-5% for alkyl nitrates. A list of VOCs measured during this study using the *in situ* GC is shown in Table 1.

Canister GC System

The analytical system and methodology used for this study are similar to those used in previous studies (Russo et al., 2010; Sive, 1998; Zhou et al., 2010). For each sample, a 1265 cm^3 (STP) aliquot of air was trapped on a glass bead filled loop immersed in liquid nitrogen. After the sample was trapped, the loop was isolated, warmed to 80 °C and injected. The carrier gas (UHP helium) flushed the contents of the loop and the stream was split into five, with each sub-stream feeding a separate GC column/detector pair as follows: (1) a CP-Al_2O_3/Na_2SO_4 PLOT column (Varian-Chrompack; 50 m × 0.53 mm i.d., 10 μm film thickness) connected to an FID was used to measure C_2-C_7 NMHCs; (2) a VF-1ms column (Varian-Chrompack; 60m × 0.32 mm i.d., 1 μm film thickness) connected to a FID measured C_4-C_{10} NMHCs; (3) a CP-PoraBond Q column (Varian-Chrompack; 25 m × 0.25mm i.d., 3 μm thickness) coupled to a Restek XTI-5 column (Restek; 30 m × 0.25 mm i.d., 0.25 μm film thickness) connected to an FID was used to measure selected OVOCs; (4) an OV-1701 column (Ohio Valley Specialty Chemical; 60 m × 0.25 mm i.d. 1 μm thickness) connected to an ECD was used to measure C_1-C_5 alkyl nitrates and C_1-C_2 halocarbons; (5) and an OV-624 column (Ohio Valley Specialty Chemical; 60 m × 0.25 mm i.d., 1.4 μm thickness) connected to an MS measured C_6-C_{10} NMHCs, C_1-C_2 halocarbons, and was used to measure select OVOCs and reduced sulphur compounds.

Trail Ridge Road Ozone Calibrations

Calibrations of the POMS unit were consistent with the US EPA guidance and were performed at Air Resource Specialists, Inc. (ARS) immediately prior to deployment and again after the campaign. The calibrations were performed by comparing the instrument output to an ultraviolet (UV) photometer transfer standard that is traceable to EPA. The instruments were

challenged at multiple O_3 concentrations (including zeros) and evaluated by the acceptance criteria which includes the percent difference of the analyser's response during the multipoint challenges and the instrument's linearity. The ARS calibration acceptance criteria for O_3 is ≤3% for the multipoint challenges and ≤1% for the linearity. Further details regarding the calibrations of the O_3 and meteorological measurements can be found in the Gaseous Pollutant Monitoring Program 2015 Quality Assurance Project Plan (https://ard-request.air-resource.com/Project/documents.aspx).

Details for calculating air mass photochemical age

The dominant source of alkyl nitrates is the photochemical production from hydrocarbons. Equations 1-6 show the chemical mechanism for alkyl nitrate production.

$RH+OH \rightarrow R+H_2O$ (k_1, α_1) (1)

$R+O_2 \rightarrow RO_2$ (k_2) (2)

$RO_2+NO \rightarrow RO+NO_2$ (k_3, $1-\alpha_4$) (3)

$RO_2+NO \rightarrow RONO_2$ (k_4, α_4) (4)

$RONO_2 + h\nu \rightarrow RO+NO_2$ (j_5) (5)

$RONO_2+OH \rightarrow$ products (k_6) (6)

k_1, k_2, k_3, k_4, k_6 are reaction rate constants, α_1 and α_4 are the reaction branching rates and j_5 is the photolysis rate constant.

$$RH \xrightarrow{k_A} RONO_2 \xrightarrow{k_B} \text{products} \quad (7)$$

$$\frac{(RONO_2)}{(RH)} = \frac{ß k_A}{(k_B - k_A)}(1 - e^{(k_A - k_B)t}) + \frac{(RONO_2)_0}{(RH)_0} e^{(k_A - k_B)t} \quad (8)$$

$k_A = k_1[OH]$, $k_B = k_6[OH] + J_5$, $ß = \alpha_1 \alpha_4$, $(RONO_2)_o/(RH)_o$ is the initial alkyl nitrate/parent hydrocarbon ratio. If $(RONO_2)_o/(RH)_o = 0$, the solution to equation describes the time evolution of the alkyl nitrate/parent hydrocarbon ratio based solely on gas phase hydrocarbon chemistry (Bertman et al., 1995).

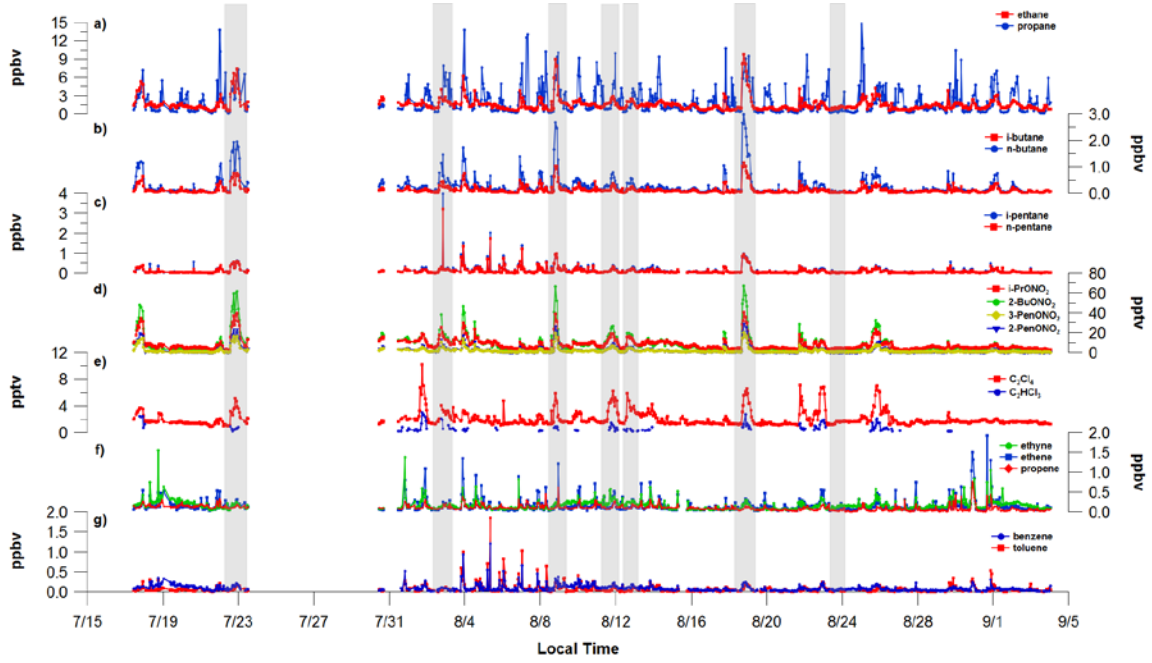

Figure S1 Time series of VOCs measured at a ROMO site during FRAPPÉ. a) ethane and propane, b) i-butane and n-butane, c) i-pentane and n-pentane, d) alkyl nitrates, e) C_2Cl_4 and C_2HCl_3, f) ethyne, ethane, and propene, g) benzene and toluene

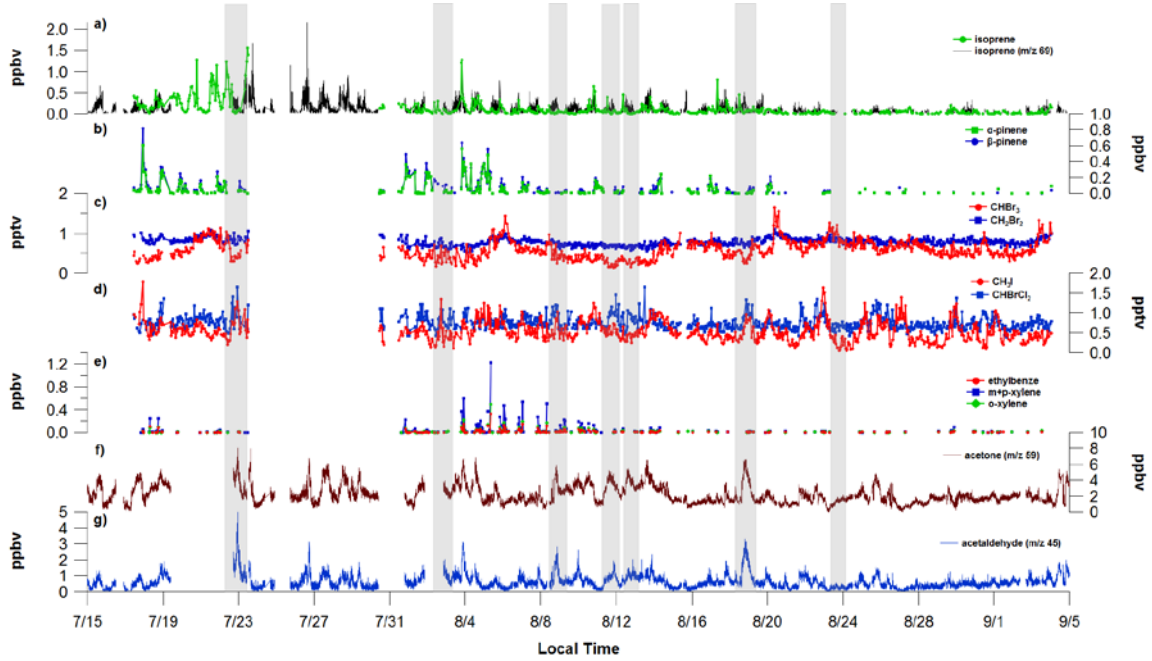

Figure S2 Time series of VOCs measured at a ROMO site during FRAPPE. a) isoprene and PTR-MS isoprene, b) α-pinene and β-pinene, c) $CHBr_3$ and CH_2Br_2, d) CH_3I and $CHBrCl_2$, e) ethylbenzene, m+p-xylene, o-xylene, f) acetone, g) acetaldehylde

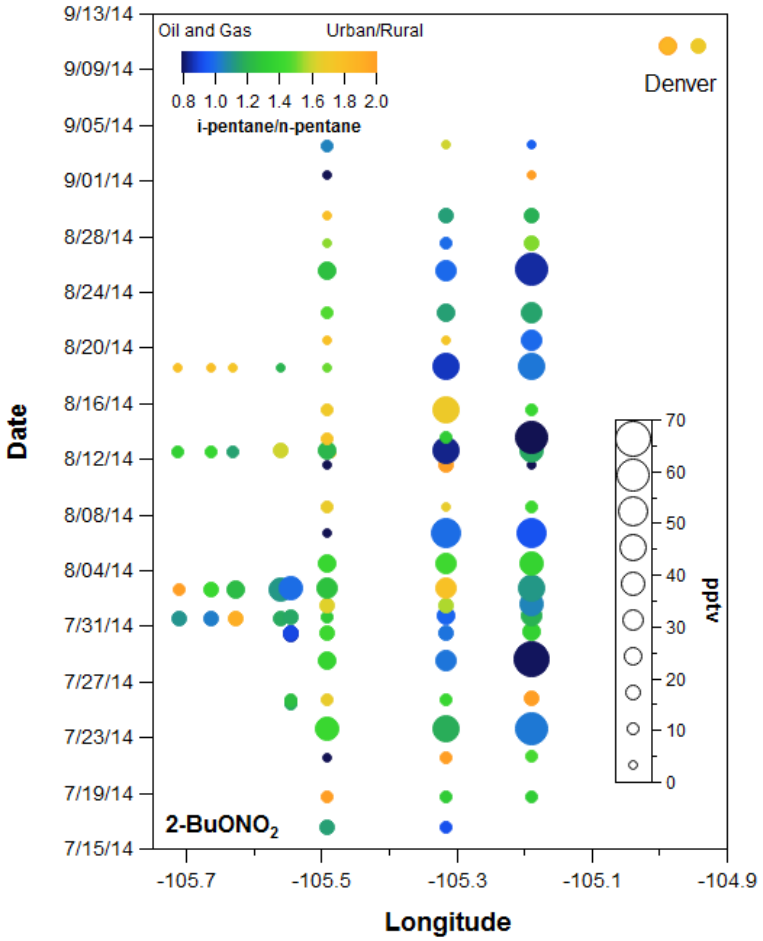

Figure S3a. VOC canister data plotted by longitude and date with 2-$BuONO_2$ mixing ratio represented by the size of each point and the i- to n-pentane represented by the colour. Locations correspond to transect samples shown in Figure 2.

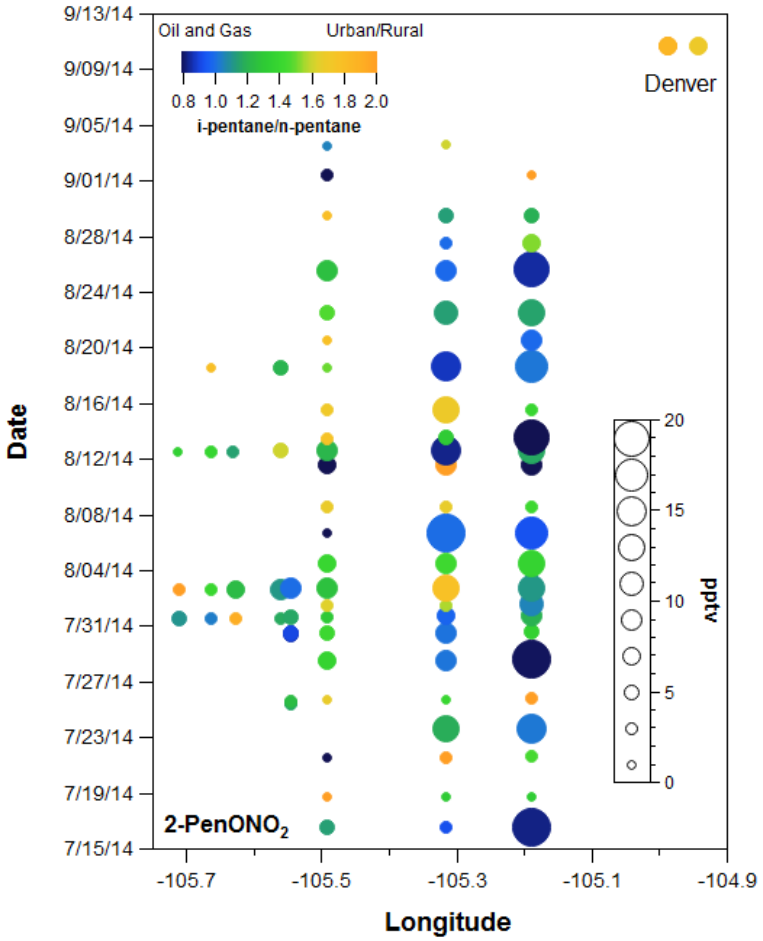

Figure S3b. VOC canister data plotted by longitude and date with 2-PenONO$_2$ mixing ratio represented by the size of each point and the i- to n-pentane represented by the colour. Locations correspond to transect samples shown in Figure 2.

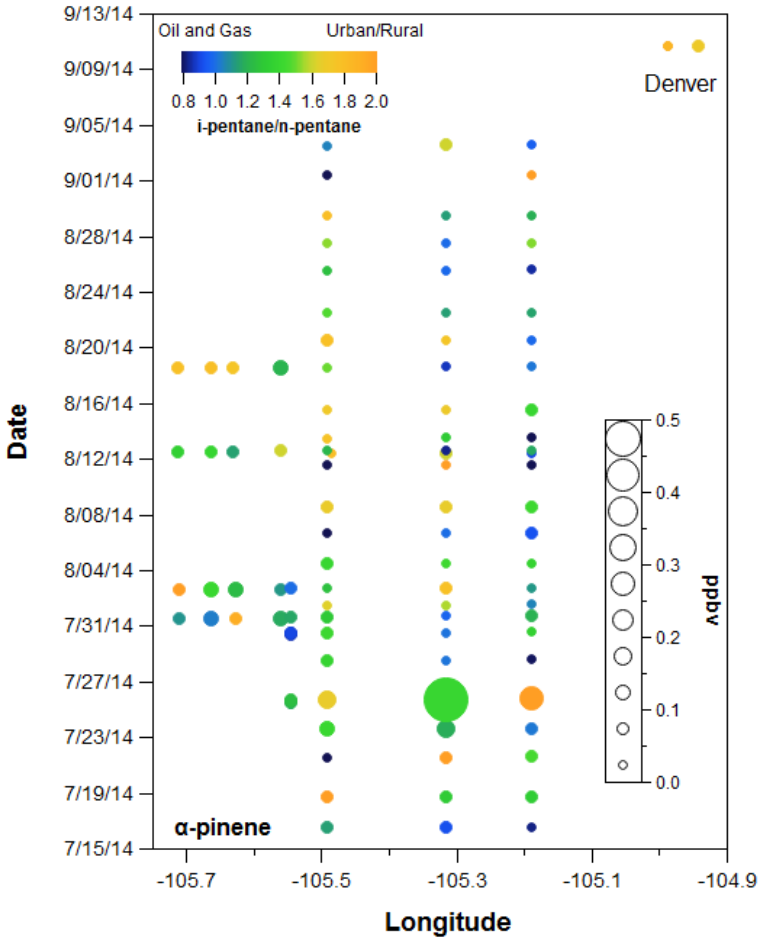

Figure S3c. VOC canister data plotted by longitude and date with α-pinene mixing ratio represented by the size of each point and the i- to n-pentane represented by the colour. Locations correspond to transect samples shown in Figure 2.

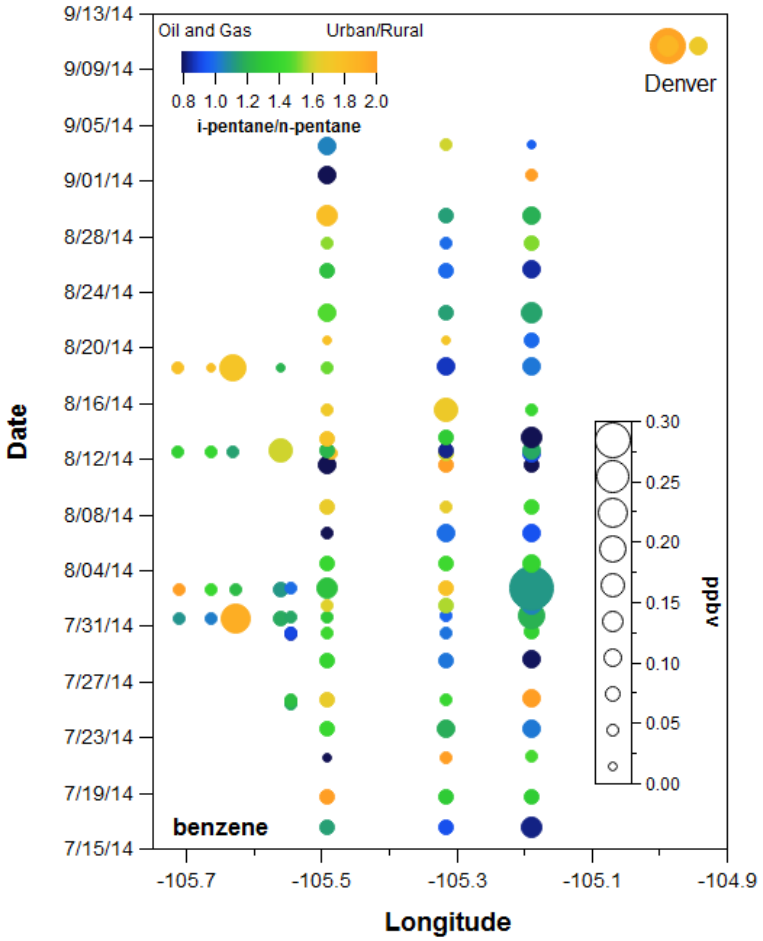

Figure S3d. VOC canister data plotted by longitude and date with benzene mixing ratio represented by the size of each point and the i- to n-pentane represented by the colour. Locations correspond to transect samples shown in Figure 2.

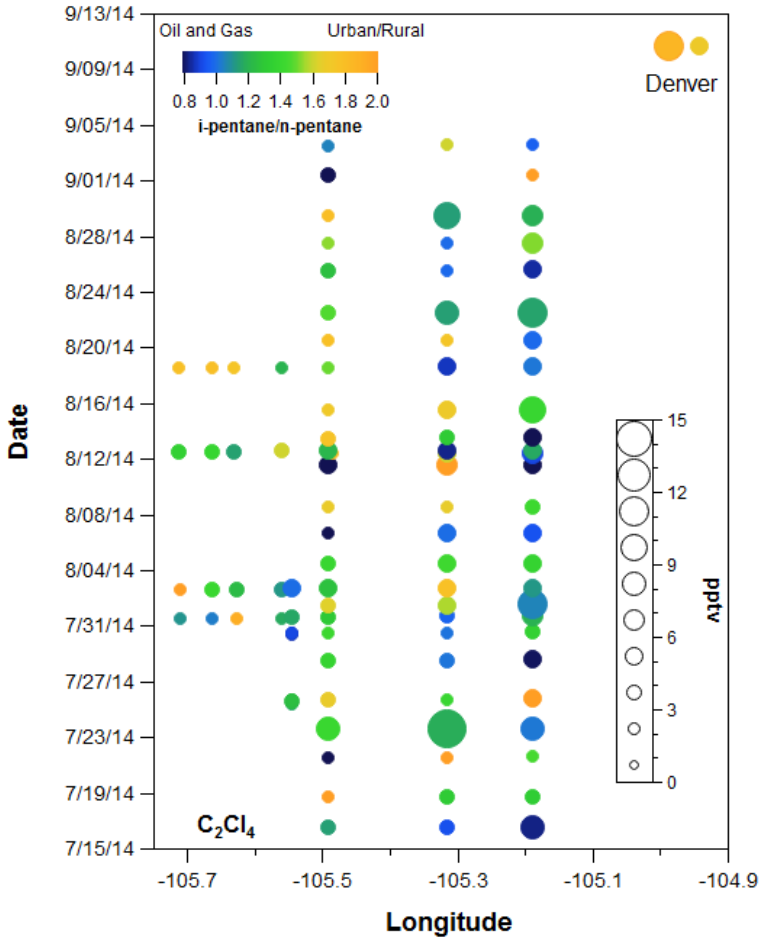

Figure S3e. VOC canister data plotted by longitude and date with C_2Cl_4 mixing ratio represented by the size of each point and the i- to n-pentane represented by the colour. Locations correspond to transect samples shown in Figure 2.

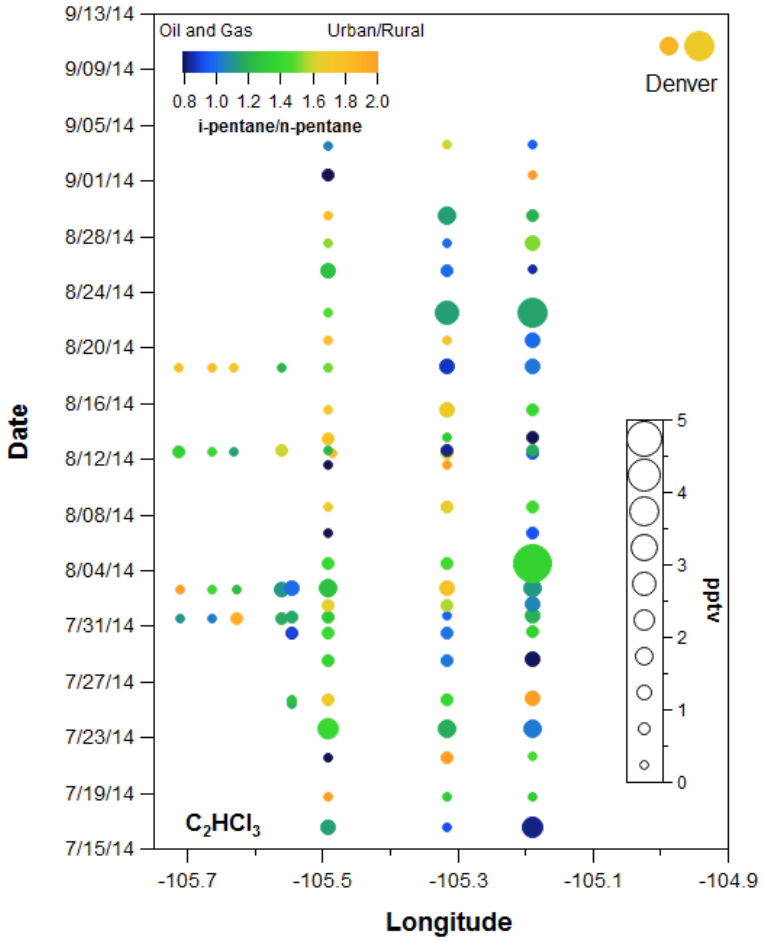

Figure S3f. VOC canister data plotted by longitude and date with C_2HCl_3 mixing ratio represented by the size of each point and the i- to n-pentane represented by the colour. Locations correspond to transect samples shown in Figure 2.

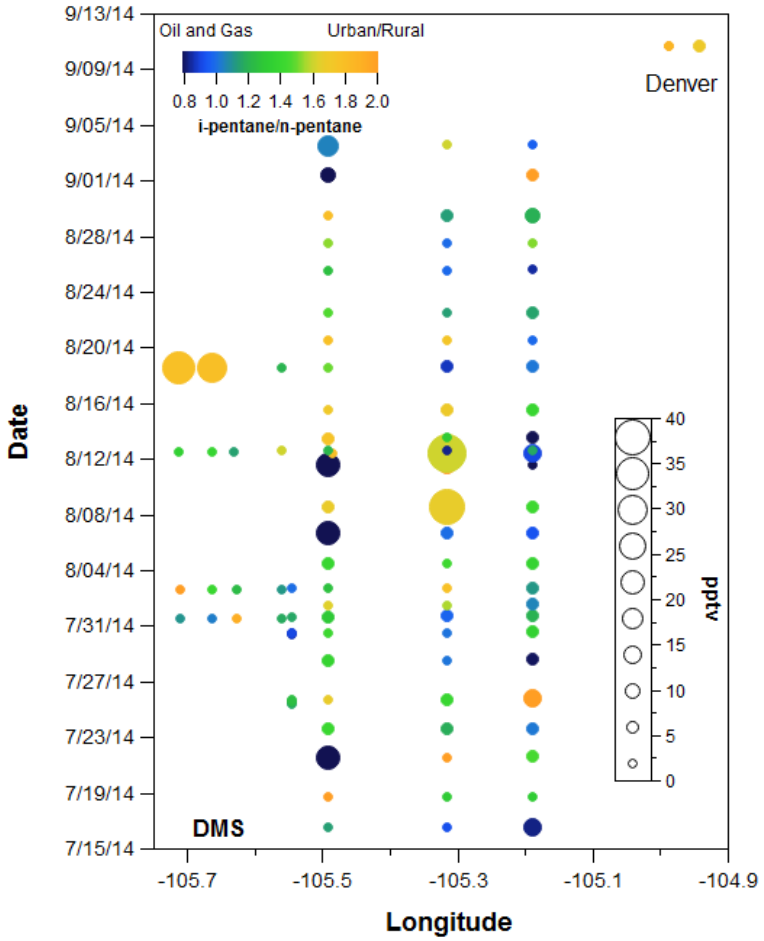

Figure S3g. VOC canister data plotted by longitude and date with DMS mixing ratio represented by the size of each point and the i- to n-pentane represented by the colour. Locations correspond to transect samples shown in Figure 2.

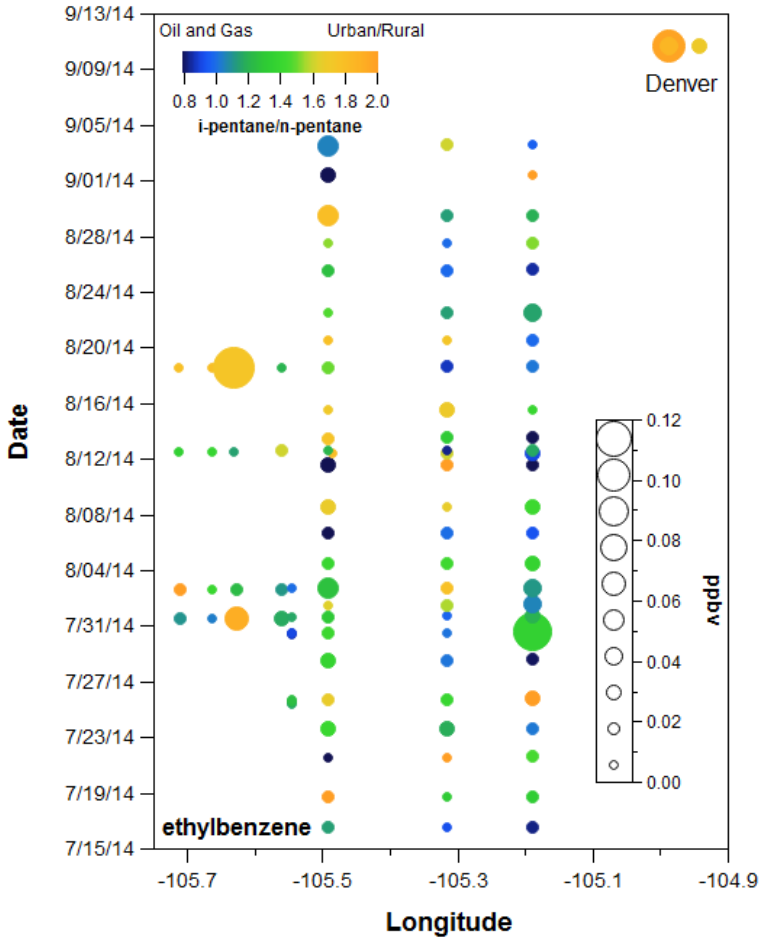

Figure S3h. VOC canister data plotted by longitude and date with ethylbenzene mixing ratio represented by the size of each point and the i- to n-pentane represented by the colour. Locations correspond to transect samples shown in Figure 2.

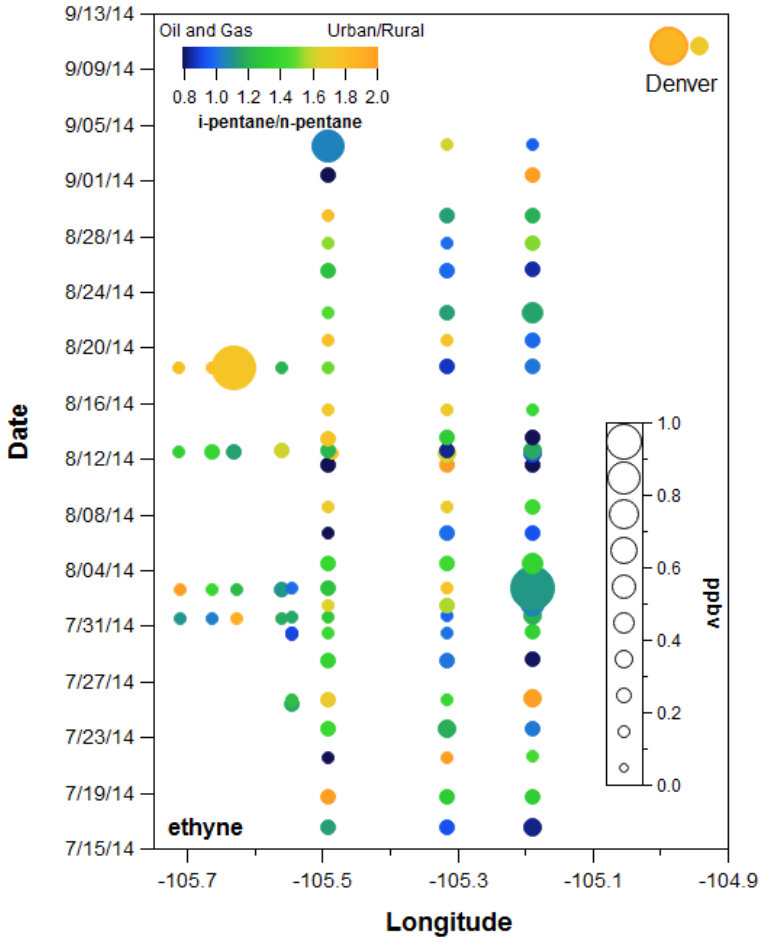

Figure S3i. VOC canister data plotted by longitude and date with ethyne mixing ratio represented by the size of each point and the i- to n-pentane represented by the colour. Locations correspond to transect samples shown in Figure 2.

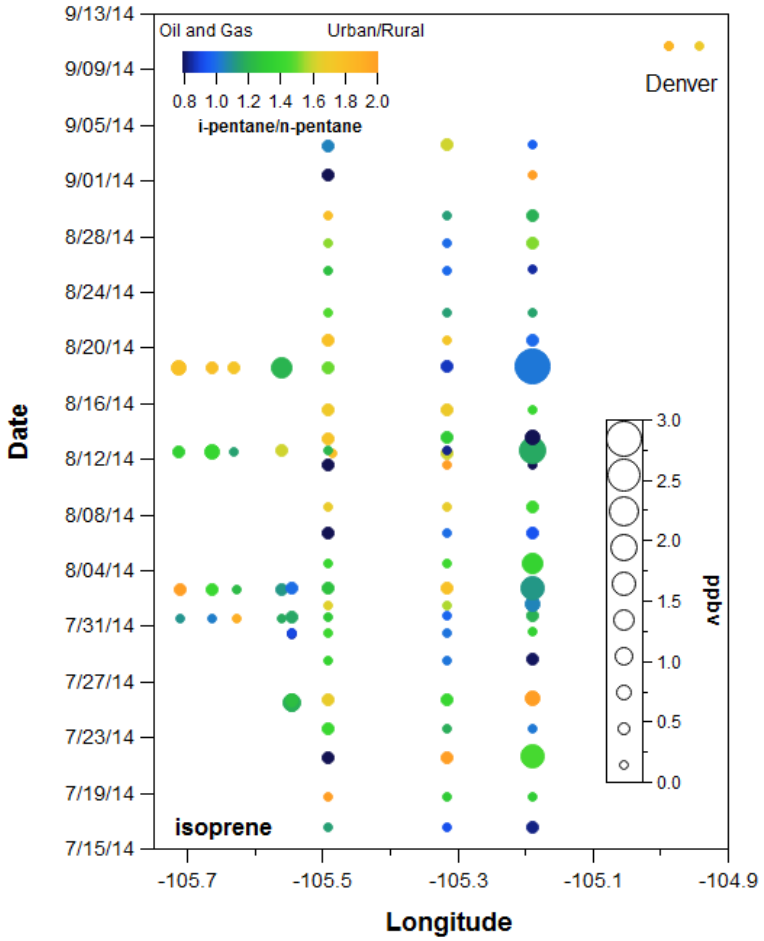

Figure S3j. VOC canister data plotted by longitude and date with isoprene mixing ratio represented by the size of each point and the i- to n-pentane represented by the colour. Locations correspond to transect samples shown in Figure 2.

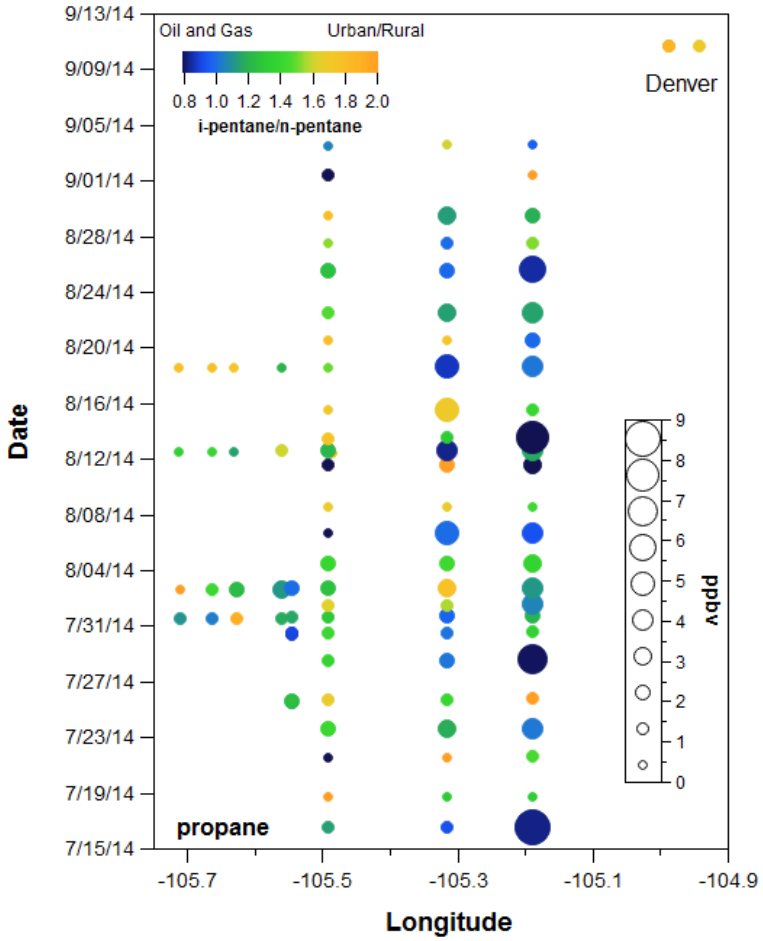

Figure S3k. VOC canister data plotted by longitude and date with propane mixing ratio represented by the size of each point and the i- to n-pentane represented by the colour. Locations correspond to transect samples shown in Figure 2.

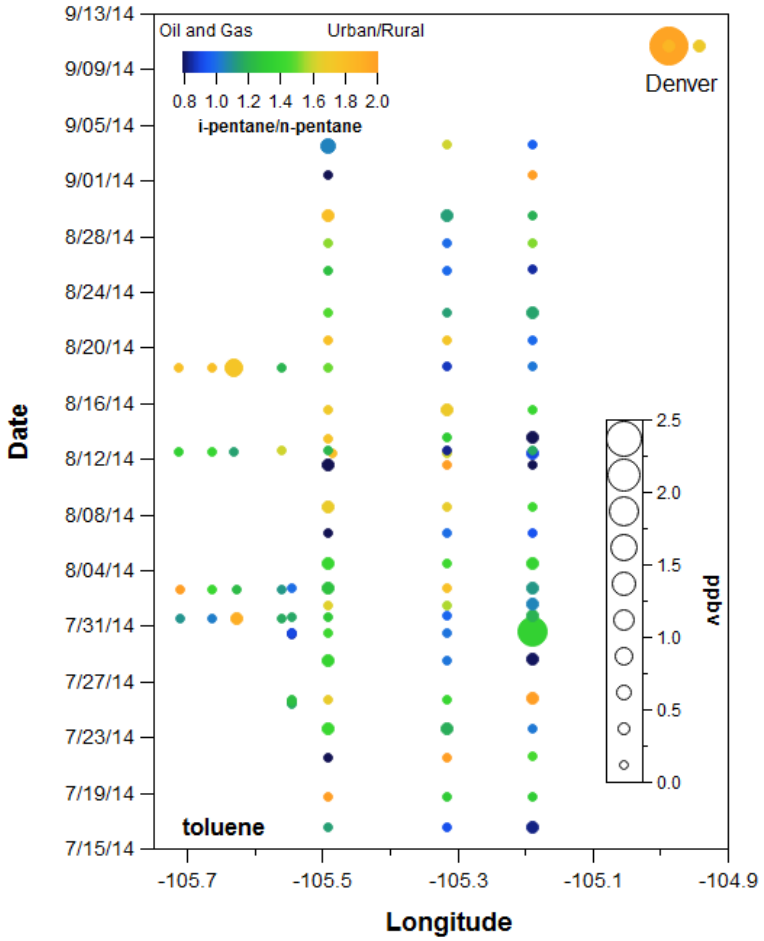

Figure S3l. VOC canister data plotted by longitude and date with toluene mixing ratio represented by the size of each point and the i- to n-pentane represented by the colour. Locations correspond to transect samples shown in Figure 2.

	Alpine Visitors Center		Forest Canyon		Rainbow Curve		Many Parks Curve		ROMO		Beaver Meadows		Eastes Park Resort		E of Drake		Big Thompson School		Camp site CDPHE (Downtown)		City Park Denver
	Average	Stdev	Average	Stdev	Average	Stdev	Average	Stdev	Average	Stdev	Average	Stdev	Average	Stdev	Average	Stdev	Average	Stdev	Average	Stdev	
ethane	1151.8	413.3	1180.1	461.6	1313.5	424.9	1694.0	845.0	1739.6	736.1	2072.9	1199.7	1600.6	825.8	2854.2	2003.5	4102.2	2885.9	2624.5	842.5	1734.0
propane	442.7	288.5	595.4	570.2	594.2	282.1	932.7	797.2	1148.7	675.2	1334.8	1214.0	826.3	674.1	1886.6	1607.7	3055.8	2513.3	1102.7	162.4	881.2
I-butane	60.1	36.5	88.4	49.7	80.2	38.3	253.6	149.0	126.6	105.5	220.6	232.2	158.0	115.9	355.0	388.1	519.6	423.8	216.3	65.4	225.4
n-butane	129.4	95.7	253.2	216.2	198.8	90.5	638.5	411.3	300.5	278.3	565.3	628.5	400.5	316.9	879.9	914.7	1390.9	1219.5	579.9	219.1	885.5
ethyne	100.5	28.9	107.2	29.5	110.3	43.0	459.8	604.9	110.3	80.2	145.5	75.3	189.3	150.4	178.4	78.0	292.8	229.4	988.0	135.1	303.0
I-pentane	43.5	22.7	260.7	395.8	71.1	26.0	629.8	589.1	97.8	72.0	239.2	218.4	362.1	385.0	436.1	577.9	512.6	334.9	687.7	464.7	395.3
n-pentane	38.7	24.6	92.6	80.3	57.4	17.3	375.0	320.0	95.1	73.2	191.7	192.8	220.8	232.5	341.9	388.8	494.2	417.4	355.6	228.3	233.8
n-hexane	13.5	9.2	28.2	14.9	17.4	5.7	175.6	177.2	26.0	18.3	58.4	41.0	65.9	71.4	87.6	90.7	136.9	105.2	153.5	96.2	82.4
n-heptane	5.5	2.3	12.3	5.9	9.7		78.1	74.8	11.2	4.1	16.8	11.9	26.9	23.3	31.7	25.8	44.5	29.2	301.8	355.0	37.0
n-nonane	16.2	4.2	15.2	6.3	16.7	9.5	42.4	12.9	24.3	12.7	20.2	7.4	23.0	10.1	25.1	13.0	27.5	10.3	37.3	26.0	17.7
benzene	22.4	7.8	34.6	13.0	26.3	11.1	123.3	92.5	31.3	9.9	82.4	71.2	62.7	34.8	63.6	34.9	102.5	71.8	231.8	117.2	107.9
toluene	17.4	6.4	38.0	28.9	26.2	8.2	339.4	400.3	34.6	14.9	75.0	45.8	114.7	95.9	77.0	50.9	198.4	382.9	1608.0	1758.6	189.9
ethylbenzene	3.1	1.4	5.5	4.7	3.2	0.7	56.4	66.5	4.0	0.9	11.7	9.8	16.4	15.2	10.0	6.2	20.9	24.5	69.7	45.5	31.2
m+p-xylene	7.9	3.9	15.8	14.4	8.8	2.7	201.9	225.7	11.4	5.0	38.1	31.3	54.1	53.0	24.9	19.7	63.6	97.9	228.1	165.1	104.2
o-xylene	3.6	1.8	7.0	6.1	4.1	1.3	76.1	82.2	5.2	1.8	14.5	11.4	20.5	18.9	11.1	7.8	23.9	26.8	85.9	61.9	37.4
styrene	2.8	1.3	3.2	2.1	1.8	0.7	6.8	3.6	3.2	0.6	4.6	4.1	3.7	2.1	4.0	3.5	5.9	6.8	12.5	7.9	5.9
Isoprene	287.6	66.6	272.7	174.3	316.3	200.6	191.2	172.9	382.1	295.1	506.9	488.2	153.8	103.6	117.8	102.3	599.9	748.1	37.9	4.5	159.2
a-pinene	49.9	31.0	45.8	7.0	81.7	27.6	69.4	44.2	44.6	17.6	80.5	40.8	34.1	31.7	53.9	128.8	34.6	58.0	4.2	2.4	36.9
b-pinene	34.6	22.7	38.5	9.1	101.9	69.0	40.9	14.4	66.7	30.0	74.3	49.5	36.6	38.8	54.3	131.3	33.4	74.0	1.2	0.8	51.1
DMS	0.7	0.2	1.2	0.2	0.6	0.3	0.9	0.2	1.0	0.4	1.6	0.2	1.7	1.3	1.8	1.3	4.0	3.2	1.0	0.1	3.2
CH_2Cl_2	35.2	3.9	37.3	3.7	36.9	6.7	37.6	8.4	30.2	5.8	35.5	4.6	33.9	5.0	36.6	4.9	46.0	41.4	37.6	1.4	38.3
C_2HCl_3	0.2	0.0	0.2	0.1	0.1	0.1	0.3	0.2	0.3	0.4	0.5	0.3	0.5	0.5	0.6	0.6	1.1	1.2	1.4	0.2	3.8
C_2Cl_4	2.1	0.4	2.1	0.5	2.6	0.6	2.6	0.6	2.2	0.9	2.7	1.1	3.0	1.4	4.5	3.1	5.6	2.7	10.3	0.9	4.6
$MeONO_2$	4.6	0.4	5.0	0.4	4.9	0.3	4.8	0.5	6.1	0.9	5.1	0.7	6.0	1.2	6.4	1.7	6.7	2.3	7.7	1.5	6.2
$EtONO_2$	2.7	0.8	3.0	1.0	3.1	0.8	3.8	1.5	4.0	1.0	3.5	1.9	4.1	2.2	5.3	2.5	6.0	2.9	6.3	2.4	3.3
$I\text{-}PrONO_2$	7.2	3.1	8.3	4.3	9.3	4.1	10.9	6.2	13.4	4.1	13.4	8.2	12.2	9.1	17.7	9.5	21.8	13.0	20.0	7.0	10.4
$n\text{-}PrONO_2$	1.6	0.7	1.8	0.8	1.8	0.6	2.2	1.0	3.0	1.4	2.6	1.1	2.8	2.3	4.0	2.4	5.1	3.2	4.6	1.7	2.2
$2\text{-}BuONO_2$	7.4	4.8	7.7	5.1	9.9	5.7	11.5	8.0	14.6	9.0	17.3	13.8	12.4	10.6	22.7	16.7	30.7	20.4	19.7	1.2	13.2
$3\text{-}PenONO_2$	1.4	0.6	2.4	1.9	2.0	0.8	3.1	2.1	3.6	2.3	4.9	2.2	3.1	2.6	5.9	4.3	7.6	4.7	5.0	0.0	2.6
$2\text{-}PenONO_2$	1.7	1.4	2.3	1.6	1.9	1.1	3.6	2.0	3.9	3.0	5.5	3.0	3.4	3.1	7.8	5.7	10.5	6.9	5.8	0.1	6.0
acetone (ppbv)	9.7	3.9	13.2	6.6	10.6	5.4	22.0	11.4	16.2	5.6	14.3	4.0	15.4	7.7	17.1	7.0	15.1	7.4	16.0	9.1	6.9

Table S1: Statistics of VOCs measured in transect samples during FRAPPE by site.

References

Abeleira, A., Pollack, I. B., Sive, B., Zhou, Y., Fischer, E. V. and Farmer, D. K.: Source characterization of volatile organic compounds in the Colorado Northern Front Range Metropolitan Area during spring and summer 2015, J. Geophys. Res. Atmospheres, 122(6), 2016JD026227, doi:10.1002/2016JD026227, 2017.

Bertman, S. B., Roberts, J. M., Parrish, D. D., Buhr, M. P., Goldan, P. D., Kuster, W. C., Fehsenfeld, F. C., Montzka, S. A. and Westberg, H.: Evolution of alkyl nitrates with air mass age, J. Geophys. Res. Atmospheres, 100(D11), 22805–22813, doi:10.1029/95JD02030, 1995.

Koppmann, R., Johnen, F. J., Khedim, A., Rudolph, J., Wedel, A. and Wiards, B.: The influence of ozone on light nonmethane hydrocarbons during cryogenic preconcentration, J. Geophys. Res. Atmospheres, 100(D6), 11383–11391, doi:10.1029/95JD00561, 1995.

Russo, R. S., Zhou, Y., Haase, K. B., Wingenter, O. W., Frinak, E. K., Mao, H., Talbot, R. W. and Sive, B. C.: Temporal variability, sources, and sinks of C1-C5 alkyl nitrates in coastal New England, Atmos Chem Phys, 10(4), 1865–1883, doi:10.5194/acp-10-1865-2010, 2010.

Sive, B. C.: Atmospheric Nonmethane Hydrocarbons: Analytical Methods and Estimated Hydroxyl Radical Concentrations, University of California, Irvine., 1998.

Sive, B. C., Zhou, Y., Troop, D., Wang, Y., Little, W. C., Wingenter, O. W., Russo, R. S., Varner, R. K. and Talbot, R.: Development of a Cryogen-Free Concentration System for Measurements of Volatile Organic Compounds, Anal. Chem., 77(21), 6989–6998, doi:10.1021/ac0506231, 2005.

Zhou, Y., Shively, D., Mao, H., Russo, R. S., Pape, B., Mower, R. N., Talbot, R. and Sive, B. C.: Air Toxic Emissions from Snowmobiles in Yellowstone National Park, Environ. Sci. Technol., 44(1), 222–228, doi:10.1021/es9018578, 2010.